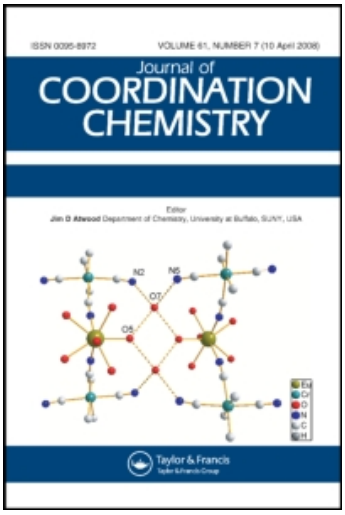

Journal of Coordination Chemistry
Publication details, including instructions for authors and subscription information:
http://www.informaworld.com/smpp/title~content=t713455674

Design, structural elucidation, DNA interaction and antimicrobial activities of metal complexes containing tetraazamacrocyclic Schiff bases

N. Raman[a]; A. Sakthivel[a]; K. Rajasekaran[a]
[a] Research Department of Chemistry, VHNSN College, Virudhunagar, Tamil Nadu, India

To cite this Article Raman, N. , Sakthivel, A. and Rajasekaran, K.(2009) 'Design, structural elucidation, DNA interaction and antimicrobial activities of metal complexes containing tetraazamacrocyclic Schiff bases', Journal of Coordination Chemistry, 62: 10, 1661 — 1676
To link to this Article: DOI: 10.1080/00958970802687554
URL: http://dx.doi.org/10.1080/00958970802687554

Journal of Coordination Chemistry
Vol. 62, No. 10, 20 May 2009, 1661–1676

Taylor & Francis
Taylor & Francis Group

Design, structural elucidation, DNA interaction and antimicrobial activities of metal complexes containing tetraazamacrocyclic Schiff bases

N. RAMAN*, A. SAKTHIVEL and K. RAJASEKARAN

Research Department of Chemistry, VHNSN College, Virudhunagar, Tamil Nadu, India

(*Received 26 June 2008; in final form 27 August 2008*)

Tetraazamacrocyclic Schiff bases, designed and synthesized from 3-hydroxy-4-nitrobenzylideneacetoacetanilide/3-hydroxy-4-nitrobenzylidene-*o*-acetoacetotoluidide and 1,2-diaminobenzene, are tetradentate ligands and form solid cationic complexes with Cu^{II}, Ni^{II}, Co^{II}, Zn^{II}, Mn^{II}, and VO^{IV} salts in ethanol. Microanalytical data, magnetic moment, electronic, IR, Mass, ^{13}C NMR, ^{1}H NMR, and electron spin resonance (ESR) techniques were used to characterize the synthesized compounds. Electronic absorption and IR spectra suggest that all the complexes are square planar, while the oxovanadium complexes are square pyramidal. Elemental analyses and mass spectra suggest that the general formula of the complexes is [ML]X (where $L = L^1$ or L^2, $X = 2Cl^-$ or SO_4^{2-}). Electrolytic behavior of the chelates was assessed from conductance data. The X-band ESR spectra of copper and oxovanadium complexes, recorded in dimethyl sulfoxide at 300 and 77 K, are discussed. Binding of the metal complexes with DNA has been investigated by spectroscopic, viscometric, and voltammetric methods. These data suggest that the complexes interact with DNA by intercalative binding. A comparative study of minimum inhibitory concentration values of the ligands and their complexes indicates that the complexes exhibit higher antimicrobial activity than the free ligands. The nuclease activity shows that the copper, manganese, nickel, and vanadium complexes cleave DNA through redox chemistry.

Keywords: Tetraazamacrocyclic complexes; Intrinsic binding constant; Redox properties; Nuclease activity; Antimicrobial activity

1. Introduction

Interactions of metal complexes with deoxyribonucleic acid (DNA) have long been the subject of intense investigation for new reagents for biotechnology and medicine. Small molecules, which react at specific sites along a DNA strand as reactive models for protein nucleic acid interactions, provide routes toward rational drug design as well as sensitive chemical probes for DNA. A number of metal complexes have been used as probes for DNA structure in solution, as agents for mediation of strand scission of duplex DNA and as chemotherapeutic agents [1–4].

*Corresponding author. Email: drn_raman@yahoo.co.in

Journal of Coordination Chemistry
ISSN 0095-8972 print/ISSN 1029-0389 online
DOI: 10.1080/00958970802687554

There has been substantial interest in rational design of transition metal complexes which bind and cleave duplex DNA with sequence or structure selectivity [5–7]. DNA recognition by small transition-metal complexes has been aided by DNA cleavage chemistry that is associated with redox-active or photo-activated metal complexes [7, 8]. The susceptibility of the ribose ring to oxidation has led to the use of a number of complexes which cleave DNA by an oxidative mechanism. Examples of such complexes include $[Fe(EDTA)]^{2-}$ [8, 9], $[Cu(phen)_2]^{2+}$ [6, 10], water-soluble metalloporphyrins [7] and the antitumor drug bleomycin [11], all of which are activated by H_2O_2 in the presence of a reductant and photoactivated $[Rh(phen)_2phi]^{3+}$ [12] and $[Rh(en)_2phi]^{3+}$ [13, 14]. Macrocyclic nickel(II) complexes with square-planar structure have been found to be effective reagents to oxidize the quinine residues in nucleic acids [15, 16]. Hence, interest is focused on the synthesis of macrocyclic complexes with potential applications in cancer diagnosis and treatment of tumors [17–19].

Condensation between dicarbonyls and primary amines has played a vital role in the development of synthetic macrocyclic ligands, a fruitful source of tetraaza macrocycles. Macrocyclic complexes of transition metal ions having aza groups show some interesting properties and biological functions such as models for metalloprotein and oxygen carrier systems [20, 21]. Dramatic progress has been achieved in the field of macrocyclic chemistry on account of its various applications in bioinorganic chemistry [22, 23]. Tetraaza macrocyclic ligands are of interest because their metal complexes function similar to porphyrin analogues in catalyzing organic reactions. Macrocyclic complexes have been found to exhibit efficient nuclease activity [24, 25], inspiring synthetic chemists to search for new metal complexes for bioactive compounds.

A literature search reveals that no work has been done on the condensation of acetoacetanilide/*o*-acetoacetotoluidide with 3-hydroxy-4-nitrobenzaldehyde and 1,2-diaminobenzene. Hence, we have designed and synthesized new macrocyclic Schiff-base ligands and their complexes using 3-hydroxy-4-nitrobenzylideneacetoacetanilide/3-hydroxy-4-nitrobenzylidene-*o*-acetoacetotoluidide and 1,2-diaminobenzene; the complexes have been characterized by analytical and spectral data.

2. Experimental

2.1. *Chemicals*

Acetoacetanilide, *o*-acetoacetotoluidide, 3-hydroxy-4-nitrobenzaldehyde, 1,2-diaminobenzene, and various metal salts were Merck products and used as supplied. Anhydrous ethanol, DMF, and dimethyl sulfoxide (DMSO) were purified according to standard procedures. Solutions of calf thymus DNA (CT DNA) in 50 mM NaCl/50 mM *tris*-HCl (pH 7.2) gave a ratio of UV absorbance at 260 and 280 nm, A_{260}/A_{280} of *ca* 1.8–1.9, indicating that the DNA was sufficiently free of protein contamination. The DNA concentration was determined by the UV absorbance at 260 nm after 1 : 100 dilution. The molar absorption coefficient was taken as $6600\,M^{-1}\,cm^{-1}$ [26]. Stock solutions were kept at 4°C and used after not more than 4 days. Doubly distilled H_2O was used to prepare the buffer. Antimicrobial activities of the ligands and their complexes were carried out by the well-diffusion method.

2.2. *Physical measurements*

^{1}H NMR, ^{13}C NMR, and microanalytical data of the compounds were recorded at the Sophisticated Analytical and Instrument Facility, Central Drug Research Institute (SAIF, CDRI), Lucknow. Fast atom bombardment mass spectrum of the complex was recorded on a JEOL SX 102/DA-6000 mass spectrometer/data system using Argon/Xenon (6 kV, 10 mA) as the FAB. The accelerating voltage was 10 kV and the spectra were recorded at room temperature using *m*-nitrobenzylalcohol (NBA) as the matrix. The IR spectra of the samples were recorded on a Shimadzu spectrophotometer from 4000 to 400 cm^{-1} using KBr pellets. The UV-vis spectra were recorded on a Shimadzu UV-1601 spectrophotometer using DMF as solvent. The X-band ESR spectra of the samples in DMSO were obtained using a Varian E112 spectrophotometer, the field being calibrated with diphenylpicrylhydrazyl (DPPH) at the SAIF, IIT Madras, Chennai. Magnetic susceptibility measurements of the complexes were carried out by Gouy balance using copper sulfate as the calibrant. The purity of ligands and their complexes was evaluated by thin layer chromatography.

Electronic spectra of the complexes were recorded before and after addition of DNA in the presence of 5 mM *tris*-HCl/5 mM NaCl buffer (pH 7.2). The intrinsic binding constant for the interaction of complex with DNA was obtained from absorption data. A fixed concentration of copper complex (10 μM) was titrated with increasing amounts of DNA over the range 20–150 μM. The equilibrium binding constant (K_b) values for the interaction of the complexes with DNA were obtained from the absorption spectral titration data using the following equation:

$$[DNA]/(\varepsilon_a - \varepsilon_f) = [DNA/(\varepsilon_b - \varepsilon_f)] + 1/K_b(\varepsilon_b - \varepsilon_f)$$

where ε_a is the extinction coefficient observed for the charge transfer absorption at a given DNA concentration, ε_f the extinction coefficient at the complex free in solution, ε_b the extinction coefficient of the complex when fully bound to DNA, K_b the equilibrium binding constant, and [DNA] the concentration in nucleotides. A plot of $[DNA]/(\varepsilon_a - \varepsilon_f)$ *versus* [DNA] gives K_b as the ratio of the slope to the intercept.

Electrochemical studies were carried out using a CH electrochemical analyzer, Model CHI620C, controlled by Chi620c software. Capacitance–voltage (CV) measurements were performed using a glassy carbon working electrode, platinum wire auxiliary electrode and a Ag/AgCl reference electrode, supporting electrolyte was 50 mM NaCl/10 mM *tris*–HCl buffer (pH 7.2). Solutions were deoxygenated by purging with N_2 prior to measurements. The molar conductances of the complexes were measured using a systronic conductivity bridge.

Viscometric experiments were carried out using an Oswald-type viscometer of 2 mL capacity thermostated in a water bath maintained at 27 ± 1°C. Flow rates of the buffer (10 mM), DNA (150 μM), and DNA in the presence of all complexes at various concentrations (5–40 μM) were measured with a manually operated time at least three times to agree within 0.2 s. The relative specific viscosity was calculated according to the relation $\eta = (t - t_0)t_0^{-1}$, where t_0 is the flow time for the buffer and t is the observed flow time for DNA in the presence and absence of the complexes. A plot of $(\eta/\eta_0)^{1/3}$ *versus* $1/R$, $R = [DNA]/[Complex]$ was constructed from viscosity measurement [27].

2.3. *Nuclease activities*

The DNA cleavage experiment was conducted using CT DNA by gel electrophoresis with the corresponding metal complex in the presence of H_2O_2 as an oxidant. Incubation of reaction mixture is performed before electrophoresis at 35°C for 2 h as follows: samples containing 30 μM CT DNA, 50 μM each complex, 50 μM H_2O_2 in 50 mM *tris*-HCl buffer (pH 7.2) were electrophoresed for 2 h at 50 V on 1% agarose gel using *tris*-aceticacid-EDTA buffer (pH 8.3). After electrophoresis, the gel was stained using 1 μg cm^{-3} ethidiumbromide (EB) and photographed under UV light using a Nikon camera.

2.4. *Antimicrobial activity*

The investigated compounds were tested against *Salmonella typhi*, *Staphylococcus aureus*, *Escherichia coli*, and *Bacillus subtilis* by the well-diffusion method [28] using agar nutrient as the medium and streptomycin as the standard. Antifungal activities of the compounds were evaluated by the well diffusion method against *Aspergillus niger*, *Aspergillus flavus*, *Candida albicans*, and *Rhizoctonia bataicola* cultured on potato dextrose agar as medium and nystatin as the standard. The stock solution (10^{-2} M) was prepared by dissolving the compounds in DMSO and the solutions were serially diluted in order to find the minimum inhibitory concentration (MIC) values. In a typical procedure [29], a well was made on the agar medium inoculated with microorganisms. The well was filled with the test solution using a micropipette and the plate was incubated, 24 h for bacteria and 72 h for fungi, at 35°C. During this period, the test solution diffused and the growth of the inoculated microorganisms was affected. The inhibition zone was developed, at which the concentration was noted.

2.5. *Synthesis of Knoevenagel condensate β-ketoanilide*

Condensation of 3-hydroxy-4-nitrobenzaldehyde (1.67 g, 0.01 mol) with acetoacetanilide/*o*-acetoacetotoluidide was performed by heating equimolar amounts (0.01 mol) under reflux in EtOH (50 mL), in the presence of five drops of piperidine as catalyst for not less than 10 h (until the solution became dark brown). The solution was then cooled and the condensate product separated by adding 30 mL of petroleum ether (40–60°C). The yellow Knoevenagel condensate *β*-ketoanilide solid that separated was filtered, washed, and recrystallized from EtOH.

2.6. *Synthesis of macrocyclic Schiff bases (L)*

3-Hydroxy-4-nitrobenzylideneacetoacetanilide (3.26 g, 0.01 mol) (L^1)/3-hydroxy-4-nitrobenzylidene-*o*-acetoacetotoluidide (3.40 g, 0.01 mol) (L^2) was dissolved in EtOH (30 mL) and refluxed with 1,2-diaminobenzene (1.08 g, 0.01 mol) in EtOH (40 mL) with the addition of 1 g of anhydrous K_2CO_3 *ca* 10 and 8 h, respectively. The solvent was reduced to one-third and the pasty mass so obtained was treated with hot

water and set aside in a refrigerator for 24 h. The solid formed was removed by filtration and recrystallized from EtOH (Supplementary Material, figure S1).

$[C_{46}H_{36}N_8O_6]$ (L^1): Yield: 80% CHN Found: C (69.1), H (4.1), N (13.9); Anal. Calcd for $[C_{46}H_{36}N_8O_6]$: C (69.3), H (4.5), N (14.0) $m/z = 796$; phenyl multiplet at 6.9–7.4 δ (m), $=C-CH_3$ at 2.4 δ (s), C–CH=C at 7.9 δ (s), Ph–NH– at 8.6 δ (s); λ_{max} in EtOH = 362 nm.

$[C_{48}H_{40}N_8O_6]$ (L^2): Yield: 54% CHN Found: C (69.4), H (4.2), N (13.1); Anal. Calcd for $[C_{48}H_{40}N_8O_6]$: C (69.8), H (4.8), N (13.5) $m/z = 824$; λ_{max} in EtOH = 300 nm.

2.7. *Syntheses of metal complexes*

A solution of $CuCl_2/NiCl_2/MnCl_2/ZnCl_2/CoCl_2/VOSO_4$ (5 mmol) and the Schiff base L^1/L^2 (5 mmol) in EtOH (50 mL) was boiled under reflux for 6 h, then concentrated to *ca* 10 mL and kept at 0°C for 24 h. The solid product formed was filtered, washed with EtOH and dried *in vacuo*.

$[CuL^1]Cl_2$: Yield: 70% [Found: Cu (6.6), C (59.1), H (3.8), N (11.9) Calcd for $[CuC_{46}H_{36}N_8O_6]Cl_2$: Cu (6.8), C (59.3), H (3.9), N (12.0)], $m/z = 930$; λ_{max} in DMF = 383 nm, 454 nm, Λm (mho cm^2 mol^{-1}) in DMF = 182, $\mu_{eff} = 1.73$.

$[NiL^1]Cl_2$: Yield: 63% [Found: Ni (6.2), C (59.5), H (3.7), N (11.8) Calcd for $[NiC_{46}H_{36}N_8O_6]Cl_2$: Ni (6.3), C (59.6), H (3.9), N (12.1)], λ_{max} in DMF = 336 nm, 471 nm, 520 nm, Λm (mho cm^2 mol^{-1}) in DMF = 158.

$[MnL^1]Cl_2$: Yield: 70% [Found: Mn (5.8), C (59.4), H (3.8), N (11.8) Calcd for $[MnC_{46}H_{36}N_8O_6]Cl_2$: Mn (5.9), C (59.8), H (3.9), N (12.1)], Λm (mho cm^2 mol^{-1}) in DMF = 125, $\mu_{eff} = 5.84$.

$[CoL^1]Cl_2$: Yield: 57% [Found: Co (6.2), C (59.4), H (3.5), N (11.9) Calcd for $[CoC_{46}H_{36}N_8O_6]Cl_2$: Co (6.3), C (59.6), H (3.9), N (12.0)], λ_{max} in DMF = 335 nm, 515 nm, Λm (mho cm^2 mol^{-1}) in DMF = 128, $\mu_{eff} = 4.79$.

$[ZnL^1]Cl_2$: Yield: 65% [Found: Zn (6.8), C (58.9), H (3.2), N (11.9) Calcd for $[ZnC_{46}H_{36}N_8O_6]Cl_2$: Zn (7.0), C (59.2), H (3.8), N (12.0)], Λm (mho cm^2 mol^{-1}) in DMF = 147.

$[VOL^1]SO_4$: Yield: 72% [Found: V (4.9), C (57.1), H (3.5), N (11.2) Calcd for $[VC_{46}H_{36}N_8O_7]Cl_2$: V (5.3), C (57.5), H (3.7), N (11.6)], λ_{max} in DMF = 272 nm, 326 nm, 596 nm, 794 nm, Λm (mho cm^2 mol^{-1}) in DMF = 97, $\mu_{eff} = 1.71$.

$[CuL^2]Cl_2$: Yield: 56% [Found: Cu (6.1), C (59.1), H (4.0), N (11.1) Calcd for $[CuC_{48}H_{40}N_8O_6]Cl_2$: Cu (6.6), C (60.1), H (4.2), N (11.6)], $m/z = 960$; λ_{max} in DMF = 378 nm, 536 nm, Λm (mho cm^2 mol^{-1}) in DMF = 154 $\mu_{eff} = 1.71$.

$[NiL^2]Cl_2$: Yield: 61% [Found: Ni (5.9), C (58.1), H (4.0), N (11.2) Calcd for $[NiC_{48}H_{40}N_8O_6]Cl_2$: Ni (6.1), C (60.4), H (4.2), N (11.7)], λ_{max} in DMF = 236 nm, 347 nm, 419 nm, 580 nm, Λm (mho cm^2 mol^{-1}) in DMF = 160.

$[MnL^2]Cl_2$: Yield: 51% [Found: Mn (5.4), C (59.8), H (3.9), N (11.5) Calcd for $[MnC_{48}H_{40}N_8O_6]Cl_2$: Mn (5.7), C (60.6), H (4.2), N (11.7)], m (mho cm^2 mol^{-1}) in DMF = 145, $\mu_{eff} = 5.97$.

$[CoL^2]Cl_2$: Yield: 65% [Found: Co (5.9), C (59.8), H (4.0), N (11.1) Calcd for $[CoC_{48}H_{40}N_8O_6]Cl_2$: Cu (6.1), C (60.3), H (4.2), N (11.7)], λ_{max} in DMF = 358 nm, 556 nm, Λm (mho cm^2 mol^{-1}) in DMF = 170, μ_{eff} = 4.84.

$[ZnL^2]Cl_2$: Yield: 70% [Found: Zn (6.4), C (59.2), H (3.9), N (11.3) Calcd for $[ZnC_{48}H_{40}N_8O_6]Cl_2$: Zn (6.8), C (59.9), H (4.1), N (11.6)], Λm (mho cm^2 mol^{-1}) in DMF = 147.

$[VOL^2]SO_4$: Yield: 84% [Found: V (4.9), C (58.1), H (3.8), N (11.1) Calcd for $[VC_{48}H_{40}N_8O_7]SO_4$: V (5.1), C (58.3), H (4.0), N (11.3)], λ_{max} in DMF = 348 nm, 455 nm, 859 nm, Λm (mhonm, Λm (mho cm^2 mol^{-1}) in DMF = 95, μ_{eff} = 1.72.

3. Results and discussion

The ligands and their complexes are stable at room temperature. The ligands are soluble in common organic solvents, but the complexes are soluble only in DMSO and DMF. All experiments of the ligand and its complexes were performed in ethanol and DMF, respectively, unless specified. Formation and purification of the ligands and their complexes were performed using chromatographic techniques. The analytical data correspond well with the general formula [ML]X, where M = Cu^{II}, Ni^{II}, Co^{II}, Zn^{II}, Mn^{II}, and VO^{IV}, L = $L^1(C_{46}H_{36}N_8O_6)$ or $L^2(C_{48}H_{40}N_8O_6)$ and X = $2Cl^-/SO_4^{2-}$. The monomeric nature of the complexes was confirmed by their magnetic susceptibility values. The molar conductance data of the chelates show that all the complexes are 1 : 2 electrolytes except [VOL]SO_4, which are 1 : 1 electrolytes.

3.1. *Mass spectra*

Mass spectra of L^1 and its copper complex $[CuL^1]Cl_2$ are used to compare their stoichiometric compositions. The molecular ion peak for the ligand is observed at 796 m/z ($C_{46}H_{36}N_8O_6$) and for its copper complex at 930 m/z $[CuC_{46}H_{36}N_8O_6]Cl_2$. The mass spectrum of $[CuL^1]Cl_2$ shows a triplet peak at 929, 930 and 931 m/z with 2.2, 4.1, and 3.5% abundances, respectively. Hence, 930 m/z may be the molecular ion peak of the complex. In this complex, one of the fragment ions exhibits a peak at 859 m/z suggesting the presence of two chloride ions. The m/z of all the fragments of L^1 and its copper complex with the relative intensities confirm the stoichiometry of the complexes as $[ML]Cl_2$. This is further supported by the mass spectra of all the complexes. Observed peaks of vanadyl complexes are in good agreement with their empirical formula as indicated from microanalytical data. Thus, the mass spectral data reinforce the conclusion drawn from the analytical and conductance values.

3.2. *Electronic absorption spectra*

The electronic absorption spectra of the ligand and complexes were recorded in DMF solution. The electronic spectra provide quick and reliable information about the ligand arrangements in transition metal complexes. The UV-Vis spectral data of the Schiff bases and their Cu^{II}, Ni^{II}, Co^{II}, and VO^{IV} complexes are given in Supplementary

Material (table S1) which includes the solvent, absorption regions, band assignments and the proposed geometry of the complexes. These values are comparable with other reported complexes [30–34].

3.3. *IR spectra*

In order to study the binding of the Schiff base to the metal in the complexes, the IR spectrum of the macrocyclic Schiff base was compared with that of its starting material which does not show any band corresponding to amino and carbonyl groups confirming the condensation of these groups [35]. The spectra of both ligands show characteristic –C=N– bands in the 1626–1650 cm^{-1} region which are shifted to lower frequencies in the spectra of the complexes (1600–1610 cm^{-1}) [36, 37]. The C–H stretching and bending vibrations appear at 2780–2890 cm^{-1} and 1460–1420 cm^{-1}, respectively. The broad band in the region 3250–3600 cm^{-1} of the IR spectra of the ligands is assigned to the –OH group. The appearance of this peak in all the spectra of the complexes indicate that the –OH group is not complexed. All the Schiff bases and complexes show an intense peak at 3050–3180 cm^{-1}, characteristic of –NH– stretching, indicating the existence of free –NH–. Bonding is also shown by new bands in the spectra of the metal complexes in the region 450–500 cm^{-1} assigned to $\nu(M-N)$ that are not observed in the spectra of the ligands. The vanadyl complexes show a band at 950–990 cm^{-1} assigned to $\nu(V{=}O)$ [38].

3.4. *NMR spectra*

The ^1H NMR spectra of L^1 and its zinc complex were recorded in $CDCl_3$ and DMSO-d_6, respectively. The ^1H NMR spectrum of L^1 shows the following signals: phenyl multiplet at 6.9 to 7.4 δ (m), =C–CH_3 at 2.4 δ (s), C–CH=C at 7.9 δ (s), Ph–NH– at 8.6 δ (s). The peak at 11.4 δ (s) is assigned to the phenolic –OH group present in the 3-hydroxy-4-nitrobenzaldehyde moiety. The presence of this peak noted for the zinc complex confirms the –OH does not complex. There is no appreciable change in other signals of the zinc complex. The ^{13}C NMR data for the macrocyclic Schiff base (L^1) and its zinc complex are given in Supplementary Material (table S2). From these data the shift in this imine carbon indicates coordination of C=N to zinc. However, all other signals of the ligand and its zinc complex $[ZnL^1]Cl_2$ show significant shifts.

3.5. *ESR spectra*

The ESR spectra of the metal chelates provide information about hyperfine structures which are important in studying the metal ion environment. The X-band ESR spectra of CuL^1 in DMSO at 300 and 77 K are shown in figure 1. The 300 K spectrum shows an isotropic pattern, expected for Cu^{2+} in solution, but the spectra for the frozen solutions show the usual anisotropic pattern as expected for powder sample. The absence of half field signal at 1600 G, corresponding to the $\Delta Ms = \pm 2$ transition, rules out a Cu–Cu interaction in the ESR spectra [39]. The spin Hamiltonian parameters of the complexes are given in table 1.

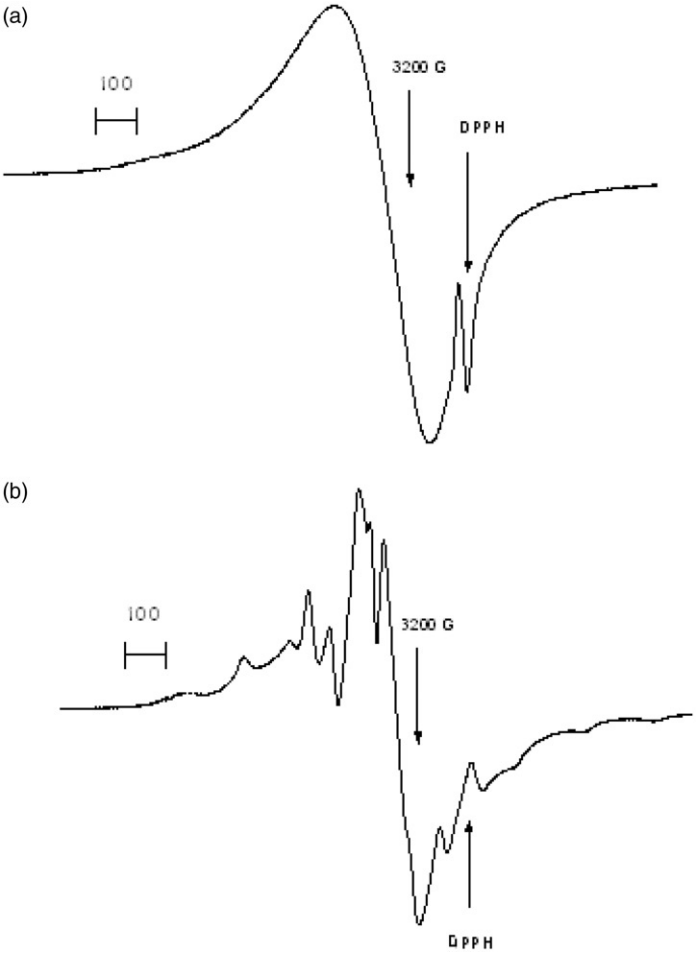

Figure 1. ESR spectrum of $[CuL^1]X$ in DMSO at (a) 300 K and (b) 77 K.

Table 1. The spin Hamiltonian parameters of Cu^{II} and VO^{IV} complexes in DMSO at 300 and 77 K.

	g-tensor			$A \times 10^{-4}\,cm^{-1}$		
Complex	$g_\perp$	$g_\parallel$	g_{iso}	$A_\parallel$	$A_\perp$	A_{iso}
$[CuL^1]Cl_2$	2.34	2.07	2.17	150	47	85
$[VOL^1]SO_4$	1.91	1.99	1.96	176	70	95
$[CuL^2]Cl_2$	2.31	2.09	2.15	170	64	79
$[VOL^2]SO_4$	1.94	1.98	1.94	168	72	94

The *g*-tensor values of the copper complex (table 1) can be used to derive the ground state. In square-planar complexes, the unpaired electron lies in the $d_{x^2-y^2}$ orbital giving $^2B_{1g}$ as the ground state with $g_\parallel > g_\perp > 2.0023$, while the unpaired electron lies in the d_{Z^2} orbital giving $^2A_{1g}$ as the ground state with $g_\perp > g_\parallel > 2.0023$. From the observed values

($g_{\parallel} > g_{\perp} > 2.0023$), it is clear that the unpaired electron lies predominantly in the $d_{x^2-y^2}$ orbital [40, 41]. The axial symmetry parameter G is defined as

$$G = \frac{g_{\parallel} - 2}{g_{\perp} - 2}$$

If G is greater than 4.0, the local tetragonal axes are misaligned parallel or only slightly misaligned. If G is less than 4.0, significant exchange coupling is present and the misalignment is appreciable. The observed values of exchange interaction parameter for the complexes ranging from 5.3 to 5.6 suggest that the local tetragonal axes are aligned parallel or slightly misaligned and the unpaired electron is present in the $d_{x^2-y^2}$ orbital. These results also indicate that the exchange coupling effects are not operative in the present complexes [41].

The ESR spectra of the vanadyl complex, recorded in DMSO solution at 300 and 77 K, show typical 8 and 16 line patterns, respectively. The room temperature (300 K) spectrum is a typical eight-line pattern, showing a single vanadium in the molecule, i.e. a monomer. In the frozen solid state, the spectrum shows two types of resonance: one set due to the parallel features and the other to the perpendicular features, showing an axially symmetric anisotropy with well resolved 16-lines hyperfine splitting characteristic of an interaction between the electron and the vanadium nuclear spin. Various parameters, calculated from the spectra of the complexes, are given in table 1. From table 1, the observed order in the parameters ($A_{\parallel} > A_{\perp}$ and $g_{\perp} > g_{\parallel}$) indicates that the unpaired electron is present in the d_{xy} orbital with square-pyramidal geometry around the oxovanadium(IV) chelates [42, 43].

Based on the above spectral and analytical data, the structures of the macrocyclic Schiff-base complexes are given in figure 2.

3.6. *DNA-binding studies*

3.6.1. Electronic absorption titration. Electronic absorption spectroscopy is often employed to ascertain the binding of complexes with DNA. Copper and zinc complexes bound to DNA through intercalation usually result in hypochromism and red shift (2–4 nm) due to the intercalative mode involving a strong stacking interaction between aromatic chromophore and the base pairs of DNA. The extent of the hypochromism is consistent with the strength of intercalative interaction [44, 45].

The electronic spectrum of $[CuL^1]^{2+}$ in the presence and absence of DNA was monitored around 385 nm, which arises due to intraligand π–π^* transition. Upon addition of incremental amounts of DNA, a considerable drop in the absorptivity of the π–π^* transition was observed. There was a moderate shift in the absorption wavelength of 4 nm on addition of DNA (Supplemental Material, figure S2). The percentage hypochromic shift of the intra-ligand band of the complex upon the binding to DNA was found to be 4% (hypochromocity, $H\% = [(\varepsilon_f - \varepsilon_b)/\varepsilon_f \times 100]$). The observed hypochromism in the absorption spectrum of the complex bound to DNA, however, was lower when compared to that of classical intercalator ethidium bromide [46]. From the plot of $[DNA]/(\varepsilon_a - \varepsilon_f)$ *versus* [DNA], the intrinsic binding constant of the complexes with DNA was calculated to be 10^4 (table 2). Moderate binding for this complex is comparable to those observed for many copper and ruthenium

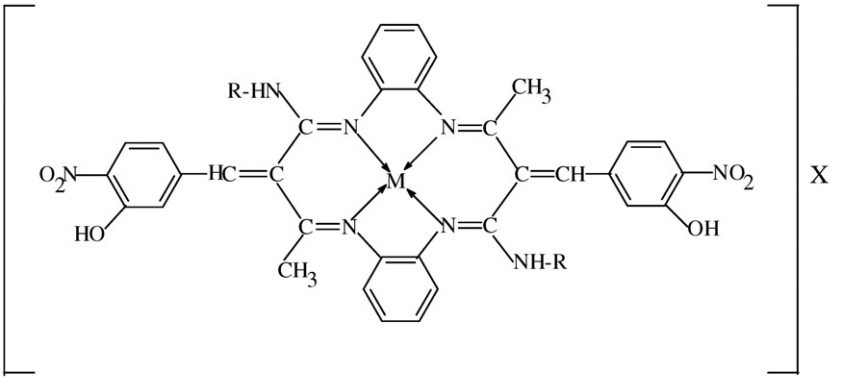

M = Cu^{II}, Ni^{II}, Co^{II}, Mn^{II} and Zn^{II}; X = $2Cl^-$

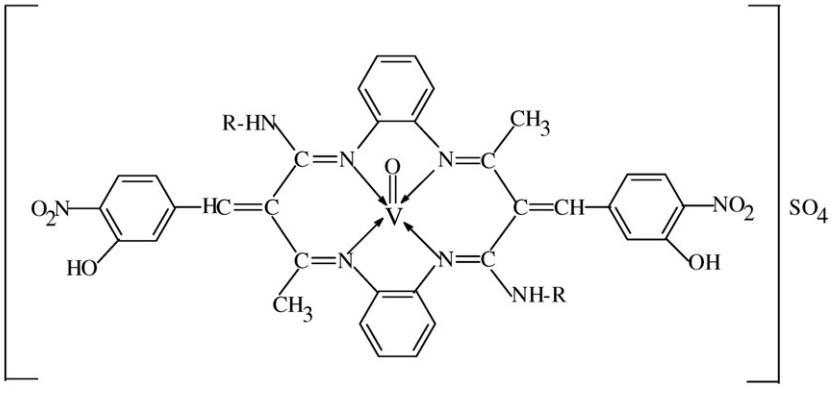

Figure 2. Proposed structure of the Schiff-base complexes.

Table 2. Absorption spectral properties of Cu^{II} and Zn^{II} complexes.

		λ_{max} (nm)				
S. No.	Complexes	Free	Bound	$\Delta\lambda$	H(%)	$K_b \times 10^4$
1	$[CuL^1]Cl_2$	383.0	380.0	3.0	4	1.25
2	$[CuL^2]Cl_2$	378.5	374.2	4.3	7	1.56
3	$[ZnL^1]Cl_2$	379.0	379.4	2.6	3	1.32
4	$[ZnL^2]Cl_2$	374.4	371.2	3.2	5	1.42

complexes [47, 48], but smaller than the classical intercalators and metallointercalators whose binding constants were of the order of 10^7.

3.6.2. Viscosity measurements. To investigate further the binding modes of the complexes, viscosity measurements on solutions of DNA incubated with the complexes were carried out. The results indicate that the presence of the complex increases the viscosity of the DNA solutions, as illustrated in figure 3. Generally, drug molecules increase the viscosity of DNA when they intercalate into the double strand DNA or

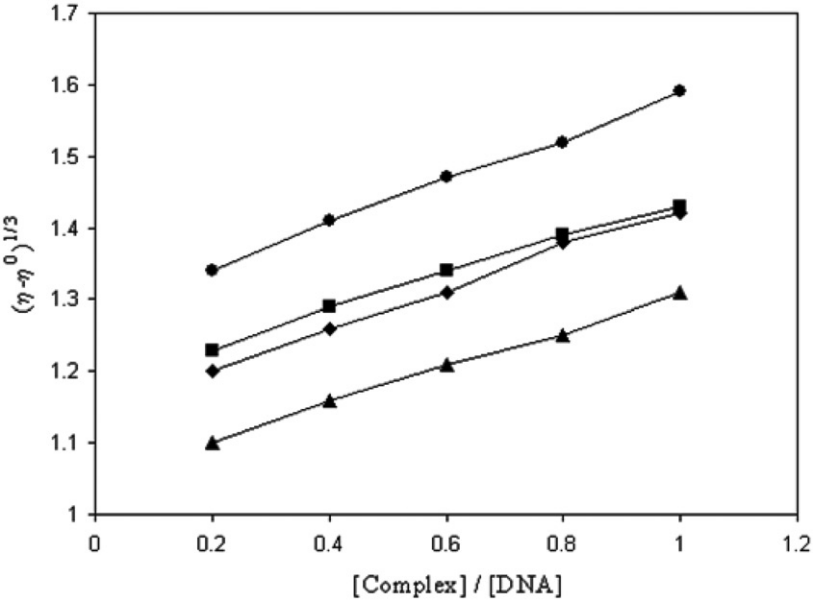

Figure 3. The effect $[CuL^1]^{2+}$ (◆), $[CuL]^{2+}$ (▲), $[ZnL^1]^{2+}$ (■) and $[ZnL^2]^{2+}$ (●), on the viscosity of DNA; relative specific viscosity *vs.* $R = [CuL]^{2+}/[DNA]$ or $[ZnL]^{2+}/[DNA]$.

bind to the phosphate group of the DNA backbone [49], the viscosity of DNA increasing the ratio of both copper and zinc complexes to DNA. This result further suggested an intercalative binding mode of the complex with DNA and paralleled the spectroscopic results, such as hypochromism and bathochromism of complexes in the presence of DNA.

3.6.3. Cyclic voltammetry. Cyclic voltammetry has been extremely useful in probing the nature and mode of DNA binding of complexes. Cyclic and differential pulse voltammetric techniques have been employed to study the interaction of the redox active copper(II) complexes with DNA to further explore the DNA binding modes. Cyclic voltammograms of $[CuL^1]^{2+}$ in the absence and presence of DNA are shown in figure 4. The cathodic peak potential (E_{pc}) and anodic peak potential (E_{pa}) in the absence of DNA are −6.9 and −5.8 V *versus* Ag/AgCl electrode, respectively. The separation of the anodic and cathodic peak potentials, ΔE_p, is 1.01 V and the ratio of cathodic to anodic peak currents, i_{pc}/i_{pa}, is 1.75, indicating a quasi-reversible redox process. The formal potential ($E_{1/2}$), taken as the average of E_{pc} and E_{pa}, is −0.63 V in the absence of DNA. Upon addition of DNA, the complex experiences a negative shift in $E_{1/2}$ of 15 mV and decrease in ΔE_p of 20 mV. The i_{pc}/i_{pa} value decreases in the presence of DNA.

Differential pulse voltammogram (DPV) of the $[CuL^1]^{2+}$ complex in the absence and presence of DNA is given in Supplemental Material (figure S3). The peak potential and current of the $[CuL^1]^{2+}$ were changed in the presence of DNA. According to the following equation [50],

$$E_b^{o'} - E_f^{o'} = 0.0591 \log(K_+/K_{2+})$$

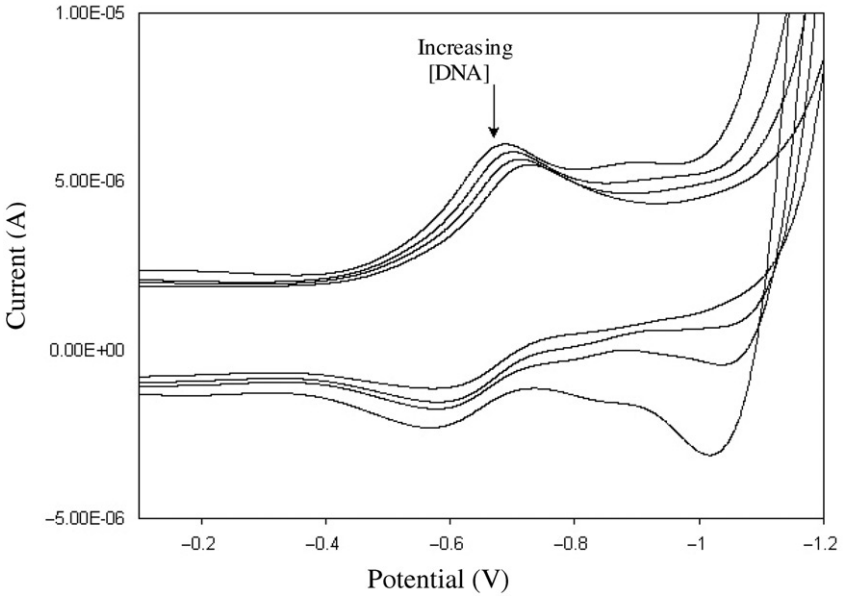

Figure 4. Cyclic voltammogram of $[CuL^1]^{2+}$ both in the absence and presence of DNA.

where $E_b^{o'}$ and $E_f^{o'}$ are formal potentials of the redox couple in the DNA bound and free forms, respectively, and K_+ and K_{2+} the corresponding binding constants for the binding of the 1+ and 2+ species to DNA, respectively [51] (table 3). K_+/K_{2+} values for the copper complexes are greater than unity suggesting preferential stabilization of Cu(I) form over Cu(II) form on binding to DNA. The possible mechanism is shown below:

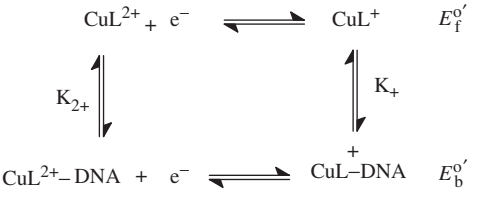

The observed cathodic peak potential for $[CuL^1]^{2+}$, the Cu^{II}/Cu^{I} reduction has been found to shift to a more positive value from −6.9 V *versus* Ag/AgCl electrode in the presence of DNA (Supplementary Material, figure S3). The 130 mV shift in the Cu^{II}/Cu^{I} potential on binding of the complex to DNA is indicative of the Cu^{II} state of the complex being more easily reducible upon binding to DNA compared to the free complex. Treatment of the electrochemical data gave a value of greater than unity for K_+/K_{2+} suggesting that the copper complex is a strong binder to DNA in the copper(I) state. In addition to the changes in formal potential upon addition of DNA, the voltammetric current decreases (figure 4), which can be attributed to slow diffusion of the metal complexes bound to the large, slowly diffusing DNA. DPV of the complexes as a function of added DNA also indicates a large decrease in current intensity with small shift in formal potential (Supplemental Material, figure S3) due to intercalative interaction.

Table 3. Electrochemical parameters for the interaction of DNA with Cu^{II} complexes.

	$E_{1/2}$ (V)		ΔEp (mV)			
Complex	Free	Bound	Free	Bound	i_{pc}/i_{pa}	K_+/K_{2+}
$[CuL^1]Cl_2$	−0.63	−0.65	101	169	−1.31	1.4
$[CuL^2]Cl_2$	−0.52	−0.56	156	111	−1.52	1.2

Table 4. Minimum inhibition concentration of the synthesized compounds against the growth of four fungi ($mg\,mL^{-1}$).

S. No.	Compound	*A. niger*	*A. flavus*	*C. albicans*	*R. bataicola*
1	L^1	65	72	58	86
2	$[CuL^1]Cl_2$	28	26	42	30
3	$[VOL^1]SO_4$	22	16	32	22
4	$[NiL^1]Cl_2$	32	20	24	20
5	$[CoL^1]Cl_2$	20	32	28	38
6	$[MnL^1]Cl_2$	24	40	18	42
7	$[ZnL^1]Cl_2$	44	52	66	72
8	L^2	74	56	66	98
9	$[CuL^2]Cl_2$	24	34	38	36
10	$[VOL^2]SO_4$	32	22	44	24
11	$[NiL^2]Cl_2$	20	28	18	20
12	$[CoL^2]Cl_2$	36	16	24	48
13	$[MnL^2]Cl_2$	18	30	28	52
14	$[ZnL^2]Cl_2$	50	46	55	62
15	Nystatin	10	8	12	14

3.7. *Antimicrobial activity*

For *in vitro* antimicrobial activity, the investigated compounds were tested against bacteria and fungi. The MIC values are summarized in tables 4 and 5. A comparative study of the ligand and its complexes (MIC values) indicates that complexes exhibit higher antimicrobial activity than the free ligand. From the MIC values, VOL is more potent than other complexes. Such increased activity of the complexes can be explained on the basis of Overtone's concept [52] and Tweedy's Chelation theory [53]. Furthermore, the mode of action of the compound may involve formation of a hydrogen bond through the azomethine group with the active center of the cell resulting in interference with the normal cell process. In general, metal complexes are more active than ligands because metal complexes serve as a vehicle for activation of ligands as the principle cyctotoxic species [54].

3.8. *DNA cleavage studies*

The cleavage efficiency of the complexes compared to that of the control is due to their efficient DNA-binding ability. The metal complexes convert super coiled DNA into open circular DNA. The general oxidative mechanisms proposed account for DNA cleavage by hydroxyl radicals *via* abstraction of a hydrogen from sugar units and

Table 5. Minimum inhibition concentration of the synthesized compounds against the growth of four bacteria ($mg\,mL^{-1}$).

S. No.	Compound	*E. coli*	*S. typhi*	*S. aureus*	*B. subtilis*
1	L^1	56	68	74	96
2	$[CuL^1]Cl_2$	18	24	38	16
3	$[VOL^1]SO_4$	34	44	24	30
4	$[NiL^1]Cl_2$	28	26	40	24
5	$[CoL^1]Cl_2$	42	18	22	44
6	$[MnL^1]Cl_2$	20	34	34	36
7	$[ZnL^1]Cl_2$	38	30	44	52
8	L^2	48	52	66	92
9	$[CuL^2]Cl_2$	22	32	44	26
10	$[VOL^2]SO_4$	30	18	20	22
11	$[NiL^2]Cl_2$	26	24	26	18
12	$[CoL^2]Cl_2$	34	46	42	30
13	$[MnL^2]Cl_2$	42	28	36	20
14	$[ZnL^2]Cl_2$	38	50	46	48
15	Streptomycin	14	18	12	10

predict the release of specific residues arising from transformed sugars, depending on the position from which the hydrogen atom is removed [55]. The cleavage is inhibited by free radical scavengers, implying that hydroxyl radical or peroxy derivatives mediate the cleavage reaction. The reaction is modulated by a metallocomplex bound hydroxyl radical or a peroxo species generated from the co-reactant H_2O_2.

The CT-DNA gel electrophoresis experiment was conducted at 35°C using our synthesized complexes in the presence of H_2O_2 as an oxidant. As can be seen from the results in figures S4 and S5 in Supplementary Material, at very low concentration few complexes exhibit nuclease activity in the presence of H_2O_2. Control experiment using DNA alone (lane 1) does not show any significant cleavage of CT-DNA even on longer exposure time. From the observed results in figure S4, we conclude that copper (lane 2), nickel (lane 3) and vanadium complexes (lane 7) cleave DNA as compared to control DNA, while other complexes (lane 5) do not cleave.

As can be seen from the results in figure S5, cobalt (lane 4) and manganese complexes (lane 5) have appreciable DNA cleavage ability over control DNA and other complexes. Further, the presence of a smear in the gel diagram indicates the presence of radical cleavage [56].

4. Conclusions

The nuclease activity of new macrocyclic metal complexes and their DNA binding have been established. Absorption titration studies indicate that the intensity of the spectral band of the complexes decreases with the addition of DNA. It is expected to be stacked between the base pairs upon the interaction of the complex with DNA. However, the small binding constant data ($K_b \approx 1.4 \times 10^4\,M^{-1}$) suggest that the complexes are moderate DNA intercalators. The intercalative binding of the complex with DNA has been further supported by cyclic voltammetric and viscometric studies. The nuclease activity of the complexes in the presence of H_2O_2 has been studied using CT-DNA. These complexes exhibit nuclease activity in the presence of peroxide.

Acknowledgments

The authors express their sincere thanks to the UGC, New Delhi for financial assistance and the Managing Board, Principal and Head of the Department of Chemistry, VHNSN College, Virudhunagar, Tamil Nadu, for their constant encouragement and providing research facilities.

References

[1] C.A. Mitsopoulou, C.E. Dagas, C. Makedonas. *J. Inorg. Biochem.*, **102**, 77 (2008).
[2] A. Sigel, H. Sigel. *Probing Nuclecic Acid by Metal Ion Complexes of Small Molecules*, Dekker, New York (1996).
[3] B.C.G. Soderberg. *Coord. Chem. Rev.*, **252**, 57 (2008).
[4] N. Farrell. *Transition Metal Complexes as Drugs and Chemotherapeutic Agents*, Dordrecht, Kluwer, Netherlands (1989).
[5] B.H. Geierstanger, M. Mrksich, P.B. Dervan, D.E. Wemmer. *Science*, **266**, 646 (1994).
[6] L.N. Ji, X.H. Zou, J.G. Liu. *Coord. Chem. Rev.*, **216**, 513 (2001).
[7] G. Pratviel, J. Bernadou, B. Meunier. *Angew. Chem. Int. Ed. Engl.*, **34**, 746 (1995).
[8] T.D. Tullius. *Ann. Rev. Biophys. Chem.*, **18**, 213 (1989).
[9] P.B. Dervan. *Science*, **232**, 464 (1986).
[10] D.S. Sigman, T.W. Bruice, A. Mazumder. *Acc. Chem. Res.*, **26**, 98 (1993).
[11] J. Stubbe, J.W. Kozarich. *Chem. Rev.*, **87**, 1107 (1987).
[12] A.M. Pyle, J.K. Barton, S.J. Lippard. *Progress in Inorganic Chemistry*, Vol. 38, Wiley, New York (1990).
[13] K.E. Erkkila, D.T. Odom, J.K. Barton. *Chem. Rev.*, **99**, 2777 (1999).
[14] T.P. Shields, J.K. Barton. *Biochemistry*, **34**, 15049 (1995).
[15] J.G. Muller, X.Y. Chen, A.C. Dadiz, S.E. Rokita, C.J. Burrows. *J. Am. Chem. Soc.*, **114**, 6407 (1992).
[16] C.J. Burrows, S.E. Rokita. *Acc. Chem. Res.*, **27**, 295 (1994).
[17] S. Ilhan, H. Temel, I. Yilmaz, M. Sekerci. *Polyhedron*, **26**, 2795 (2007).
[18] Y.H. Su, J. Liu, J. Li, X.Z. Si. *J. Mol. Struct.*, **837**, 257 (2007).
[19] S.G. Kang, N. Kim, J.H. Jeong. *Inorg. Chim. Acta*, **361**, 349 (2008).
[20] S. Srinivasan, P.R. Athappan, G. Rajagopal. *Transition Met. Chem.*, **26**, 588 (2001).
[21] J. Liu, T.B. Lu, H. Deng, L.N. Ji. *Transition Met. Chem.*, **28**, 116 (2003).
[22] Y.G. Fang, J. Zhang, S.Y. Chen, N. Jiang, H.H. Lin, Y. Zhang, X.Q. Yu. *Bioorg. Med. Chem.*, **15**, 696 (2007).
[23] X.Y. Wang, J. Zhang, K. Li, N. Jiang, S.Y. Chen, H.H. Lin, Y. Huang, I.J. Ma, X.Q. Yu. *Bioorg. Med. Chem.*, **14**, 6745 (2006).
[24] D.M. Kong, J. Wang, L.N. Zhu, Y.W. Jin, X.Z. Li, H.X. Shen, H.F. Mi. *J. Inorg. Biochem.*, **102**, 824 (2008).
[25] N. Sengottuvelan, D. Saravanakumar, M. Kandaswamy. *Polyhedron*, **26**, 3825 (2007).
[26] M.E. Reichmann, S.A. Rice, C.A. Thomas, P. Doty. *J. Am. Chem. Soc.*, **76**, 3047 (1954).
[27] G. Cohen, H. Eisenberg. *Biopolymers*, **8**, 45 (1969).
[28] O.N. Irobi, M.M. Young, W.A. Anderson. *Int. J. Pharm.*, **34**, 87 (1996).
[29] M.J. Pelczar, E.C.S. Chan, N.R. Krieg. *Microbiology*, 5th Edn, MacGraw-Hill Book Co., New York (1998).
[30] R.K. Lonibala, T.R. Rao, R.K. Babitadevi. *J. Chem. Sci.*, **118**, 327 (2006).
[31] A.A. Tak, F. Arjmand, S. Tabassum. *Transition Met. Chem.*, **27**, 741 (2002).
[32] B.N. Figgis, J. Lewis. *Modern Coordination Chemistry*, Wiley-Interscience, New York (1960).
[33] Y. Dong, L.F. Lindoy, P. Turner, G. Wei. *J. Chem. Soc., Dalton Trans.*, 1264 (2004).
[34] A.P. Mishra, L.R. Pandey. *Indian J. Chem.*, **44A**, 1800 (2005).
[35] K. Nakamoto. *Infrared Spectra of Inorganic and Coordination Compounds*, 4th Edn, Wiley-Interscience, New York (1986).
[36] T.L. Yang, W.W. Qin. *Indian J. Chem.*, **45A**, 2035 (2006).
[37] R. Grag, M.K. Saini, N. Fahmi, R.V. Singh. *Indian J. Chem.*, **44A**, 2433 (2005).
[38] R.K. Lonibala, T.R. Rao, R.K. Babithadevi. *J. Chem. Sci.*, **118**, 327 (2006).
[39] A.L. Sharma, I.O. Singh, H.R. Singh, R.M. Kadam, M.K. Bhide, M.D. Sastry. *Transition Met. Chem.*, **26**, 532 (2001).
[40] R.N. Patel, N. Singh, V.L.N. Gundla. *Indian J. Chem.*, **45A**, 614 (2006).

[41] A.M.F. Benial, V. Ramakrishnan, R. Murugesan. *Spectrochim. Acta*, **56A**, 2775 (2000).
[42] K.M. Kadish, D. Sazou, C. Araullo, Y.M. Liu, A. Saoiabi, M. Ferhat, R. Guilard. *Inorg. Chem.*, **27**, 2313 (1988).
[43] S.S. Dodwad, R.S. Dhamnaskr, P.S. Prabhu. *Polyhedron*, **8**, 1748 (1989).
[44] S.A. Tysoe, R.J. Morgan, A.D. Baker, T.C. Strekas. *J. Phys. Chem.*, **97**, 1707 (1993).
[45] T.M. Kelly, A.B. Tossi, D.J. McConnell, T.C. Strekas. *Nucleic Acid Res.*, **13**, 6017 (1985).
[46] M.J. Waring. *J. Mol. Biol.*, **13**, 269 (1965).
[47] J.G. Liu, B.H. Ye, Q.L. Zhang, X.H. Zou, Q.X. Zhen, X. Tian, L.N. Ji. *J. Biol. Inorg. Chem.*, **5**, 119 (2000).
[48] X.H. Zou, B.H. Ye, H. Li, Q. Zhang, H. Chao, J.G. Liu, L.N. Ji, X.Y. Li. *J. Biol. Inorg. Chem.*, **6**, 143 (2001).
[49] Y. Li, Y. Wu, J. Zhao, Y. Pin. *J. Inorg. Biochem.*, **101**, 283 (2007).
[50] C.V. Kumar, E.H. Asuncin. *J. Am. Chem. Soc.*, **115**, 8547 (1993).
[51] A.J. Bard, M.T. Carter, M. Rodriguez. *J. Am. Chem. Soc.*, **111**, 8901 (1989).
[52] Y. Anjaneyula, R.P. Rao. *Synth. React. Inorg. Met.-Org. Chem.*, **16**, 257 (1986).
[53] N. Dharamaraj, P. Viswanathamurthi, K. Natarajan. *Transition Met. Chem.*, **26**, 105 (2001).
[54] D.H. Petering. In *Metal Ions in Biological Systems*, H. Sigel (Ed.), Vol. 2, Marcel Dekker, New York (1973).
[55] G. Prativel, M. Pitie, J. Bernadou, B. Meunier. *Angew. Chem. Int. Ed. Engl.*, **30**, 702 (1991).
[56] A.M. Thomas, A.D. Naik, M. Nethaji, A.R. Chakravarty. *Indian J. Chem.*, **43A**, 691 (2004).